Optimization of plasma heating efficiency in fusion systems through suppression of energetic particle instabilities

authors:

J. Varela, D. Spong, L. Garcia, Y. Ghai, J. Ortiz-Luengo, R. Sanchez, V. Tribaldos, R. Solis, J.M. Reynolds-Barredo, J.A. Mier

Another co -author participating in FAR3d project:

ORNL: D. Del Castillo

TJ-II: C. Hidalgo, A. Cappa, S. Melnikov, E. Ascacibar

DIII-D: M. Van Zeeland, A. M. Garofalo, D. Pace, W. W. Heidbrink, X. Du

PPPL: M. Podesta, J. Breslau

NIFS & CFQS: K.Y. Watanabe, K. Nagaoka, S. Ohdachi, Y. Takemura, Y. Todo, T. Tokuzawa, K. Ida, A. Shimizu, R. Seki, Y. Suzuki

Heliotron J: K. Nagasaki, S. Kobayashi

JT60SA: K. Shinohara, J. Shiraishi, S. Yamamoto, M. Honda

EAST & CFETR: J. Huang, V. Chan, X. Wang

JET: S. Sharapov, S. Mazzi, J. Garcia

Laboratoire M2P2 CNRS: D. Zarzoso, H. Betar

Seville University: M. Garcia-Muñoz, J. Rueda.

INDEX

Project overview: What is an Alfven mode?

- Shear Alfven waves: transverse electromagnetic waves that propagates along the magnetic field lines.

- Dispersion relation of shear Alfven waves: $\omega = k_{\|} v_A$

$\omega \equiv$ wave frequency

$k_{\|} \equiv$ wave vector

$v_A \equiv$ Alfven velocity

- If the periodicity of the fusion device is included: $k_{\|} = \dfrac{n - mq}{R}$

- Waves satisfying the dispersion relation are part of the **Alfven continuum**.

- **Periodic variation of the Alfven velocity causes gaps in the continuum !!**

- **Alfven eigenmodes (AE) can be destabilized in the gaps** because there is no energy transfer towards the continuum: **exponential growth of the perturbation !!**

Project overview: Why AE stability is an important problem?

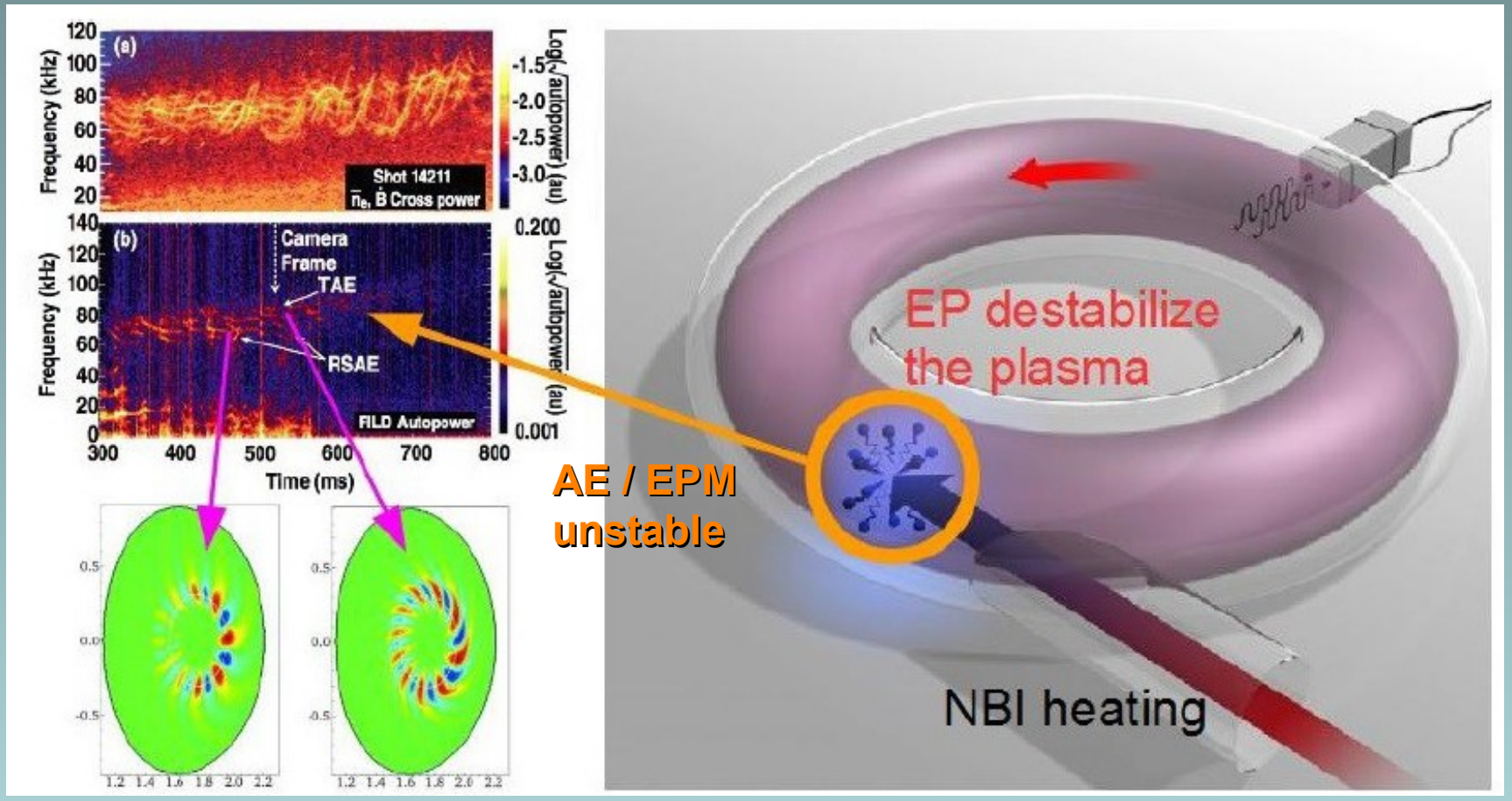

Alfven Eigenmodes unstable → Inefficient plasma heating

Only if you can heat the plasma you can have a fusion reactor !!

Project overview: the destabilization of AEs must be avoided

- **Energetic particle (EP) driven instabilities** can **enhance** the **transport** of fusion produced **alpha particles**, energetic neutral beam particles (**NBI driven EP**) and particles heated using ion cyclotron resonance heating (**ICRF driven EP**).

- **This is bad ?** **YES**

EP/alphas are lost before thermalization.

- **Consequences ?**

→ **Damage** of plasma-facing components.

→ **Inefficient** plasma heating.

→ **Increase** of the operation scenario **requirements**.

→ **Reduce or hamper** the **economic viability** of future nuclear fusion **reactors**.

Project overview: the FAR3d code

- Gyro fluid FAR3d code: thermal plasma + EP perturbation

  - Reduced MHD + Momentums of the gyro-kinetic equation (Landau closure -> kinetic eq. truncation).

  - Pressure/current gradient driven modes + wave-particle resonance effect reproducing the Landau damping\growth.

- FAR3d code main features (linear and non linear):
  - 3d system (VMEC equilibria).
  - Toroidal and helical couplings.
  - Experimental profiles as input.
  - Multiple EP species.
  - Finite Larmor Radius and e-i Landau damping effects.
  - Eigensolver: sub-dominant modes.
  - Passing (tangential NBI) and trapped (perpendicular NBI) EPs.

Project overview: why a gyro-fluid code?

- Short simulation time (minutes for serial linear simulations):
  - **Parametric studies.**
  - **Fast experimental data interpretation.**

- Optimization:
  - NBI operational regime (EP β, energy and deposition region).
  - Magnetic field topology (NBI current drive and ECCD).
  - Multiple EP population: **Multiple EP damping effects.**
  - Thermal plasma density / temperature.

- Experiment interpretation:
  - AE characterization: AE family, dominant modes, eigenfunction, ...
  - Stability trends.
  - Dominant and sub-dominant modes.
  - Saturation phase: bursting, chirping, zonal flow, zonal currents, ...

Project overview: gyro-fluid vs gyro-kinetic

- Gyro-fluid and gyro-kinetic approaches are complementary !!

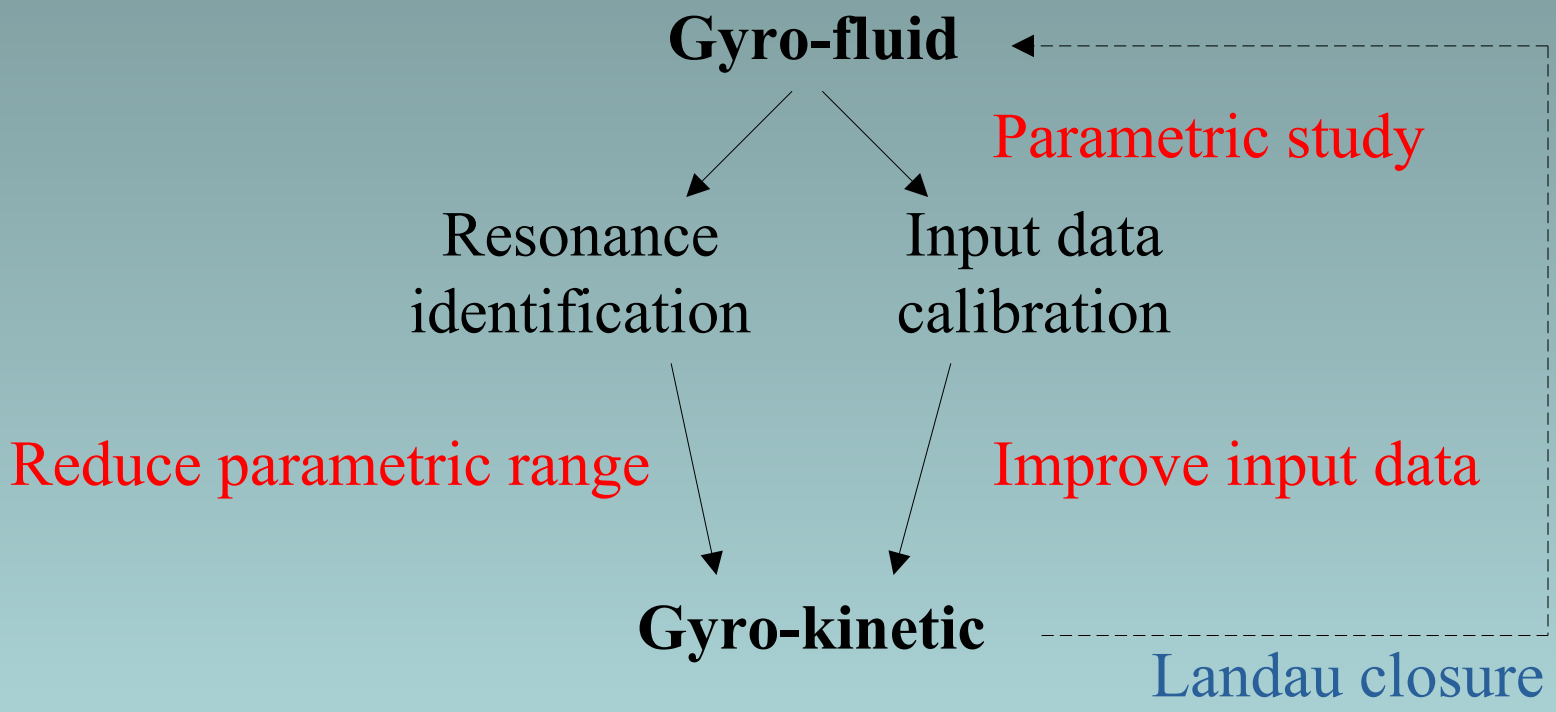

AE mode identification: consistent with observations

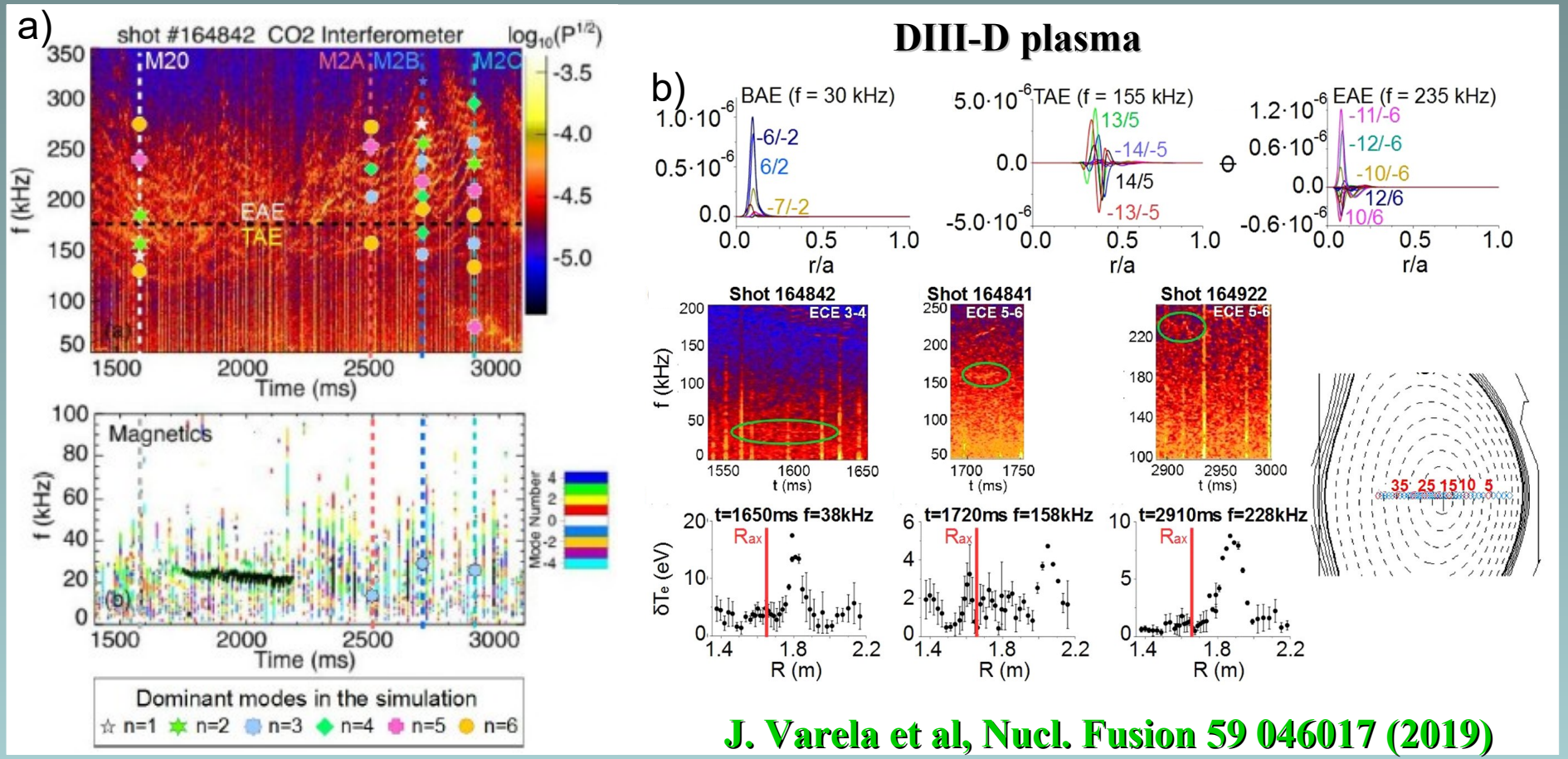

J. Varela et al, Nucl. Fusion 59 046017 (2019)

- Analysis of the AE activity along the discharge (a).
- Simulation AE frequency range, radial location, eigenfunction structure and dominant modes must be consistent with the observations (b).

Neutral beam current drive changes AE/PGDM stability

LHD plasma

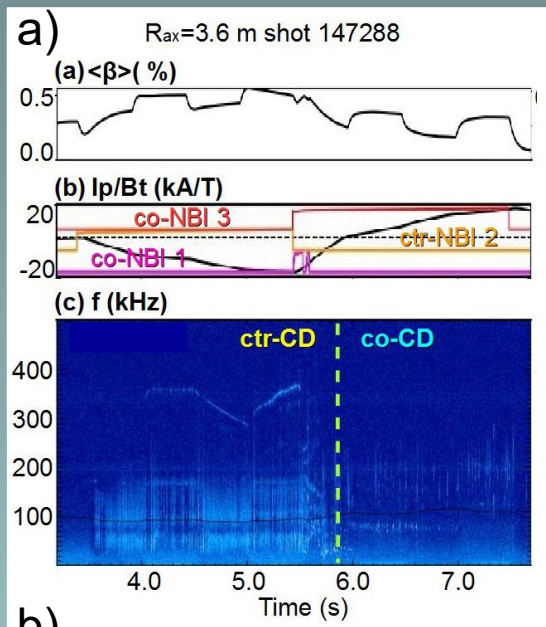

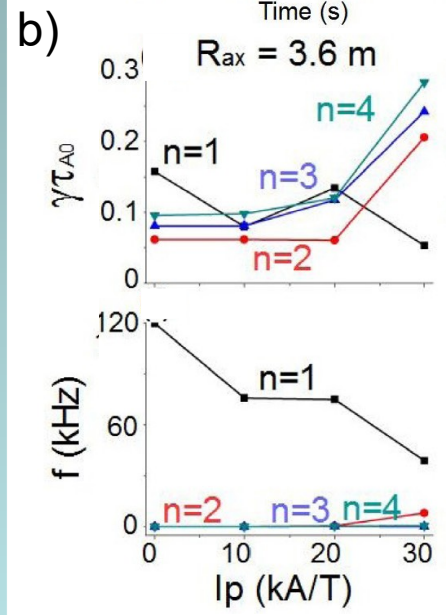

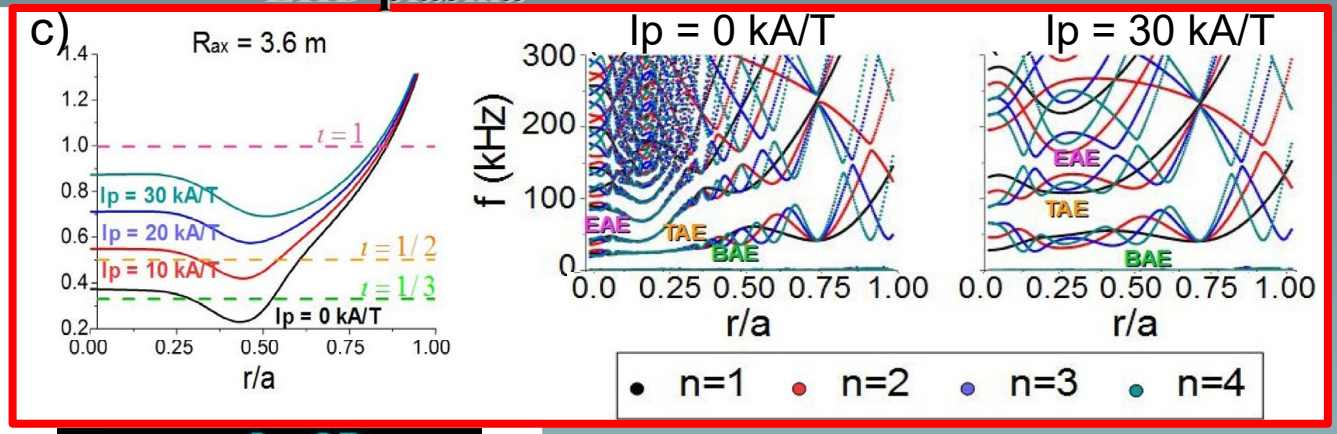

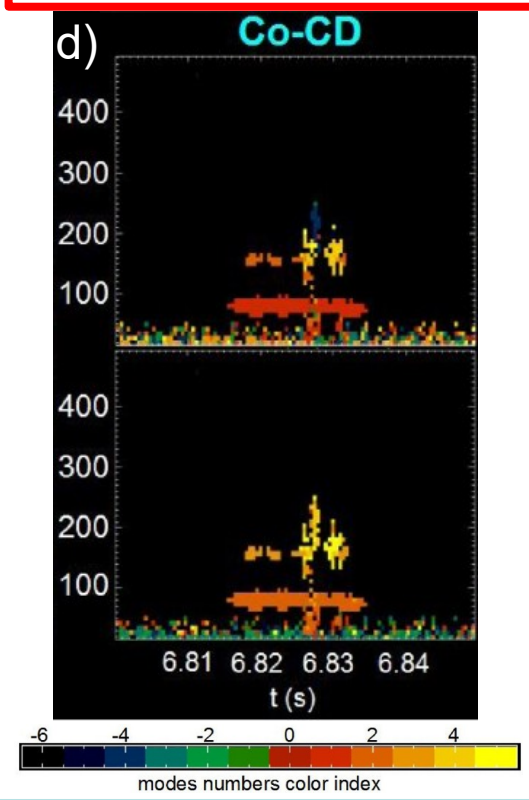

- AE stability improves during the co-NBCD phase (a).
- Simulations reproduce the same experimental stability trends (b).
- NBCD modifies the iota profile and the structure of the continuum gaps !! (c)
- AE identified consistent with experimental data (d).

J. Varela et al, Nucl. Fusion 60 026016 (2020)

NBCD control leads to AE stabilization

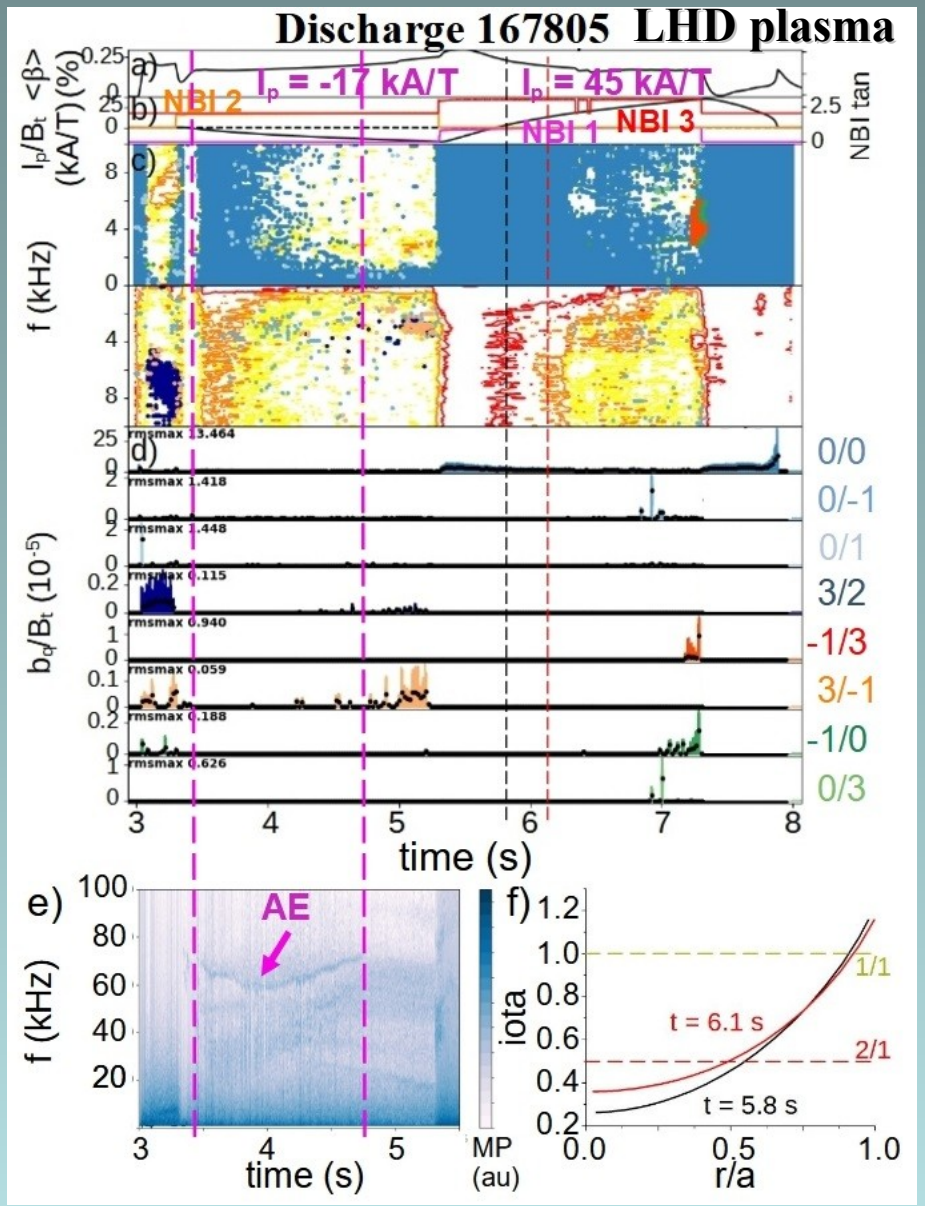

J. Varela et al, ISHW (2021)

- AE activity is observed at the beginning of the ctr-NBCD phase (b and e).

- Pressure gradient driven modes (PGDM) stable, low β (a, c and d).

- The iota profile down-shifts along the ctr-NBCD phase, leading to a iota minima below 0.2 (f).

- AE stable if ctr-NBCD intensity is above 20 kA (b and e) from t = 4.7 s.

- Down sweeping of the AE frequency caused by screening currents (iota profile up-shit) from t =3.3 to 4 s (e).

- Up sweeping of AE frequency caused by the ctr-NBCD (iota profile down-shift) from t = 4 to 5 s (e).

Slender continuum gaps induced by ctr-NBCD

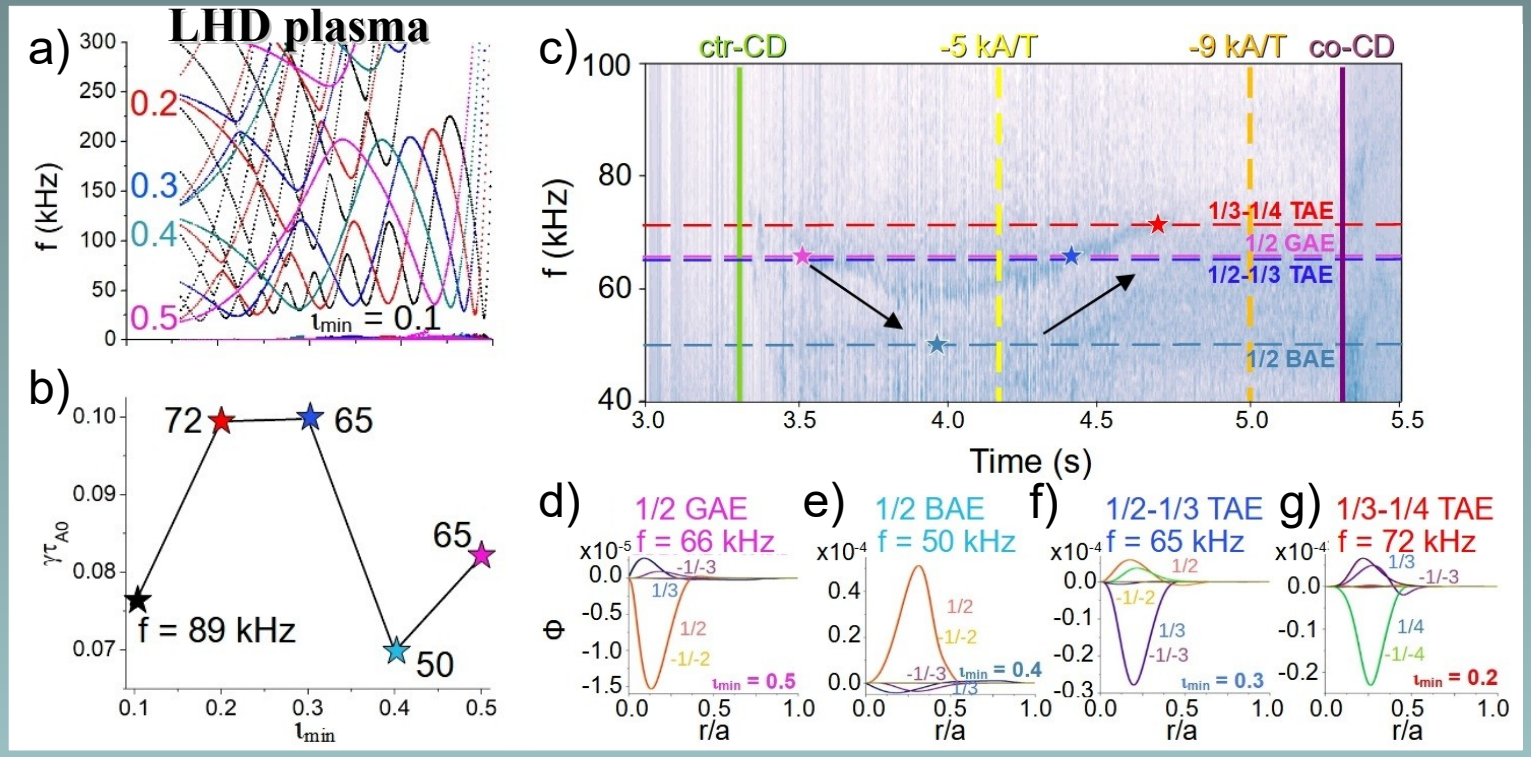

- Down-shift of the iota profile leads to a configuration with slender continuum gaps. AE growth rate decreases !! (panel a and b)

- The simulations reproduce the AE frequency down and up sweeping as the iota profile up / down shift by the screening currents and NBCD (panel c).

- The dominant AE in the simulations evolves from a 1/2 GAE (ι_{min}=0.5) to a 1/2-1/3 TAE if ι_{min}=0.3 and a 1/3-1/4 TAE if ι_{min}=0.2 (d to g).

A larger thermal plasma density leads to slender gaps

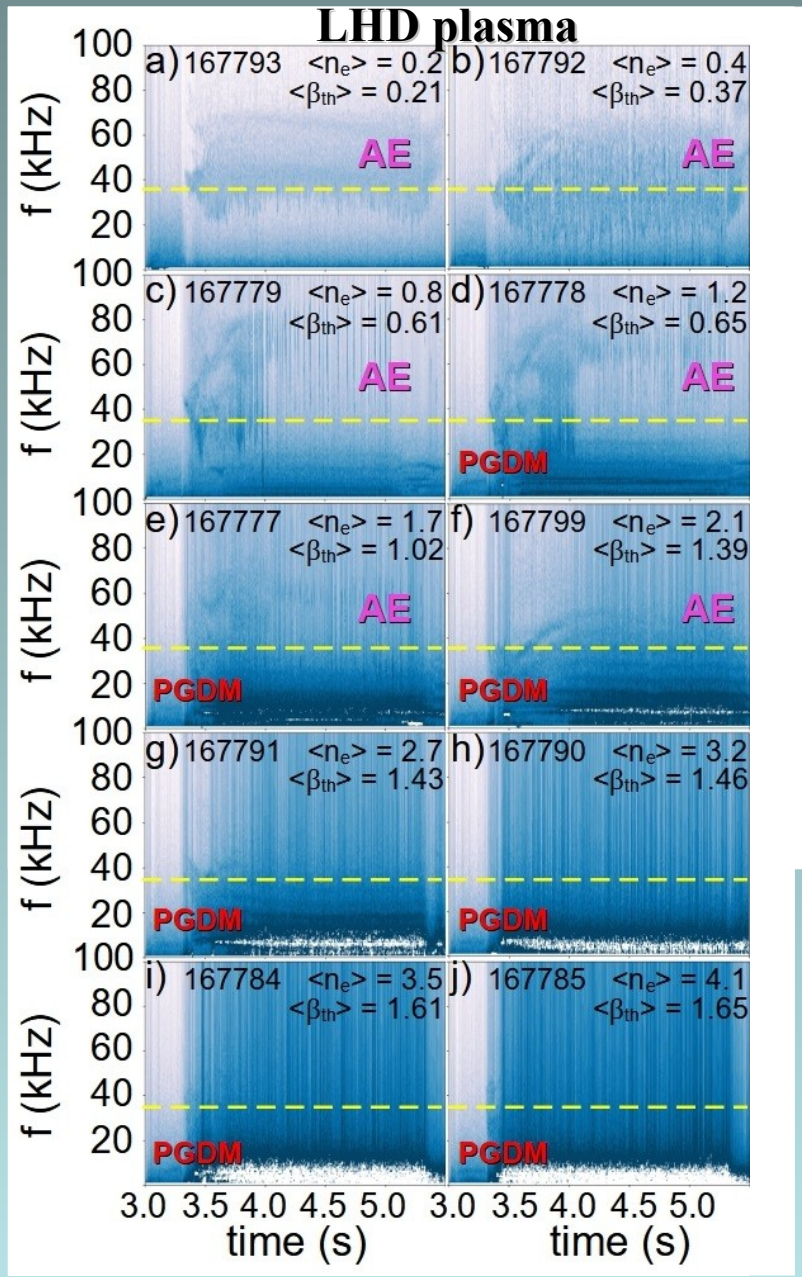

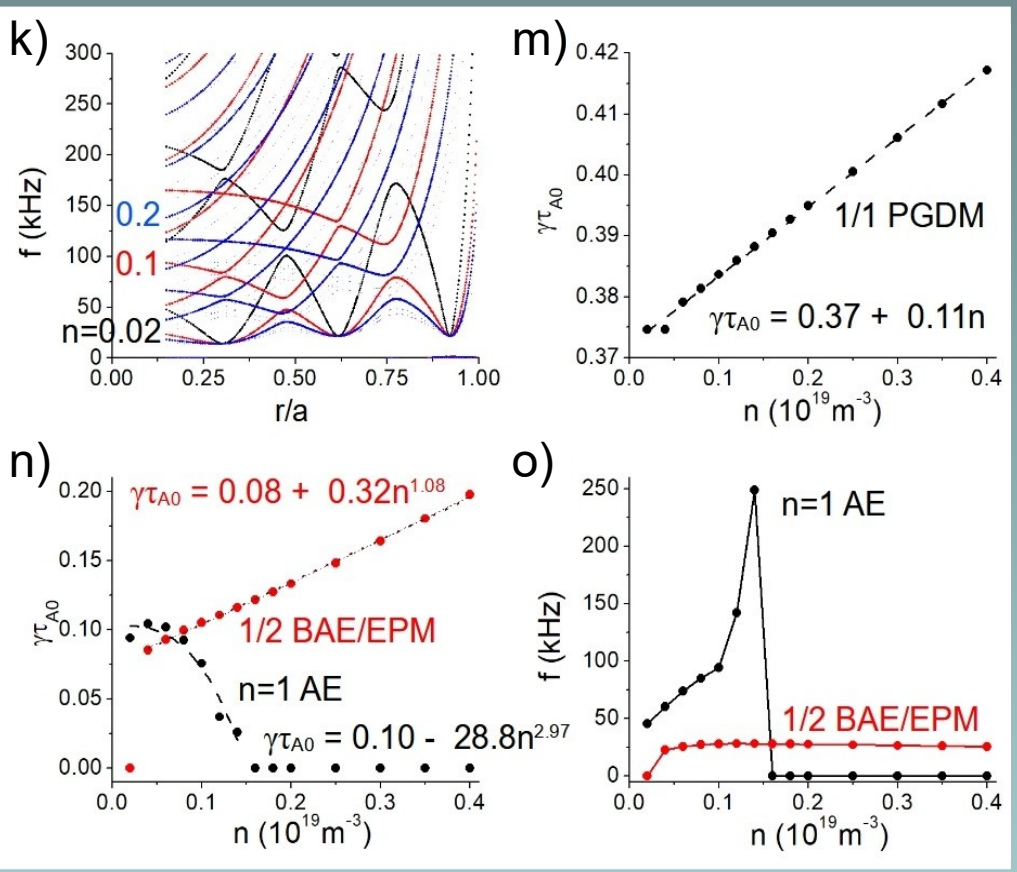

- AEs stable if the thermal plasma density is larger than $2.1 \cdot 10^{19} m^{-3}$ (a to j).

- A larger thermal plasma density leads to slender continuum gaps and improved AE stability !! (k to o).

Optimized discharges show improved MHD stability

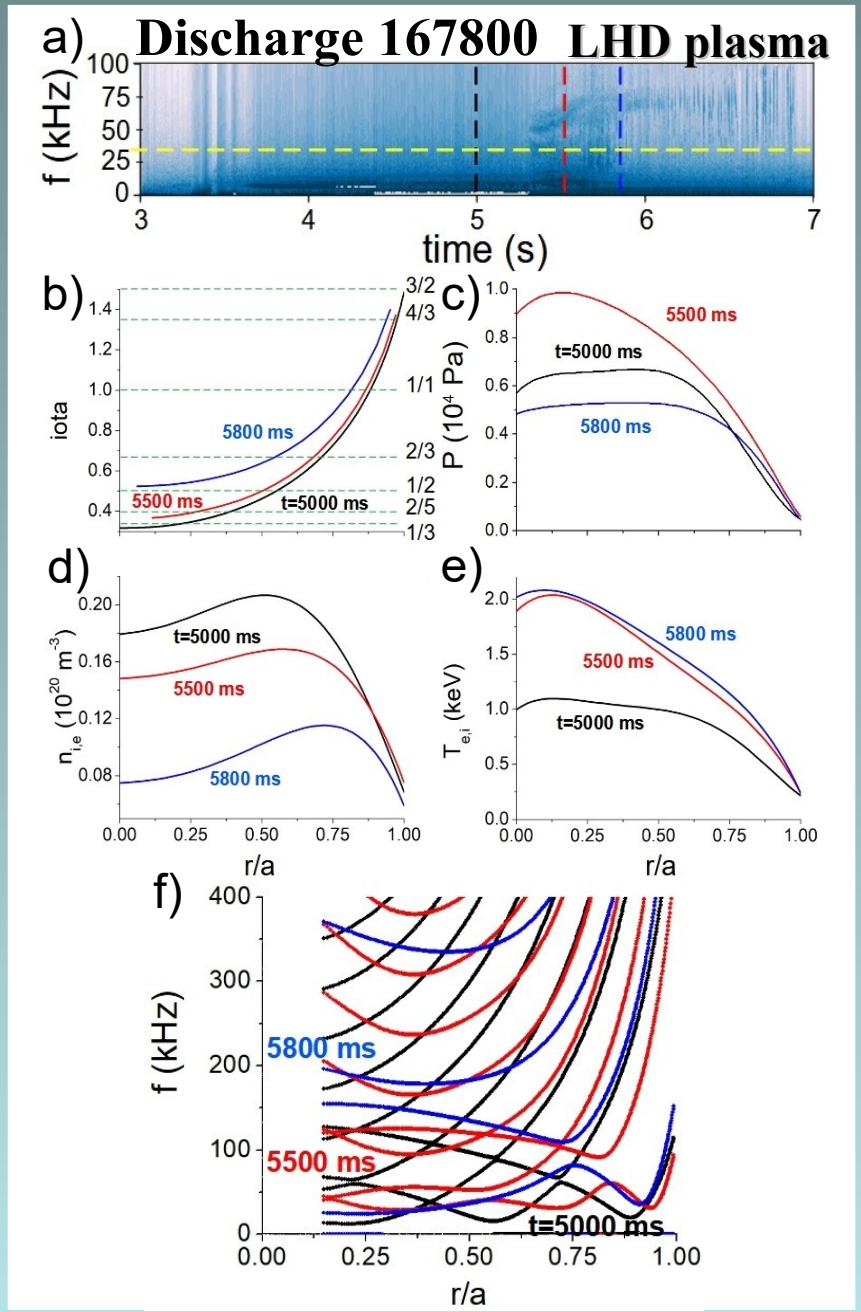

- **Optimized discharge by the control of the NBCD and plasma density: AE and PGDM stable !!** (a).

- Iota profile up-shift, plasma density decrease and temperature increase (constant thermal β) (b to e).

- Iota up-shift partially compensates the plasma density decrease avoiding the opening of a wide TAE gap (f).

Off-axis NBI injection may lead to weaker AE activity

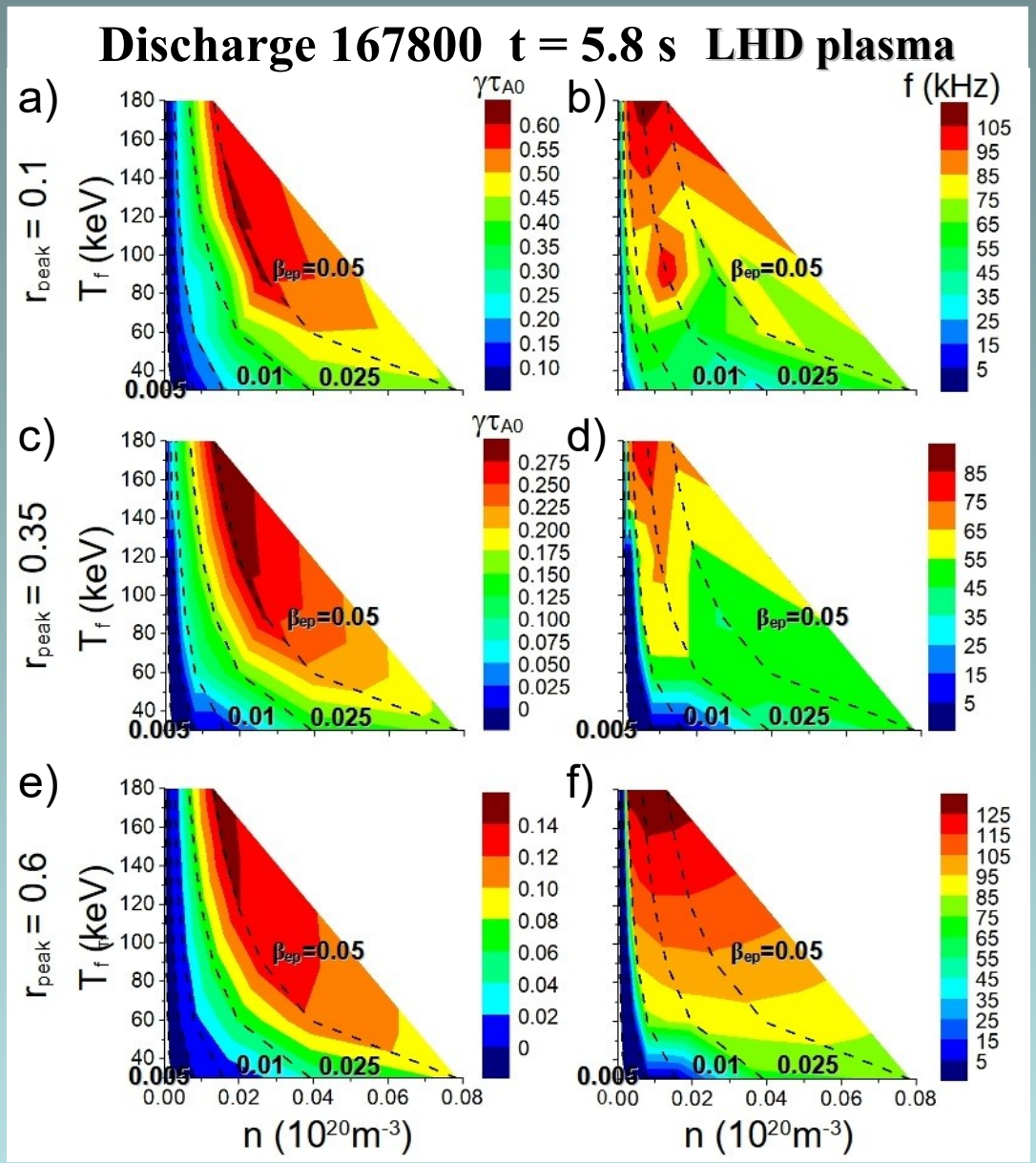

- Simulations indicate on-axis NBI injection leads to the AEs with the largest growth rates (a to b).

- Off-axis NBI injection shows a lower AEs growth rate: 2 times smaller for r/a = 0.35 (c and d), 4 times smaller for r/a = 0.6 (e to f).

- **Off-axis NBI injection has a EP β threshold 2 times larger than on-axis NBI.**

- EP populations with high energy leads to the destabilization of AEs with the largest growth rate.

On-axis ctr-ECCD can stabilize AE in LHD plasma

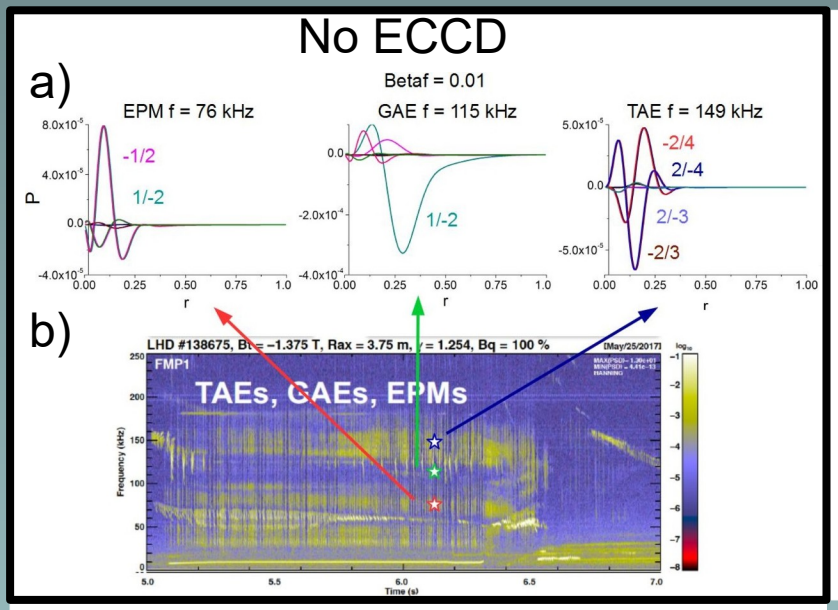

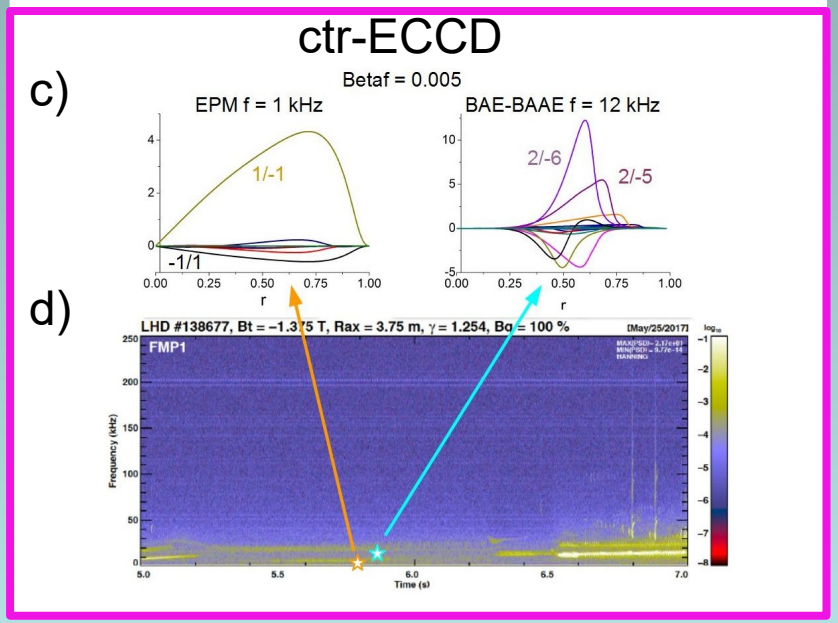

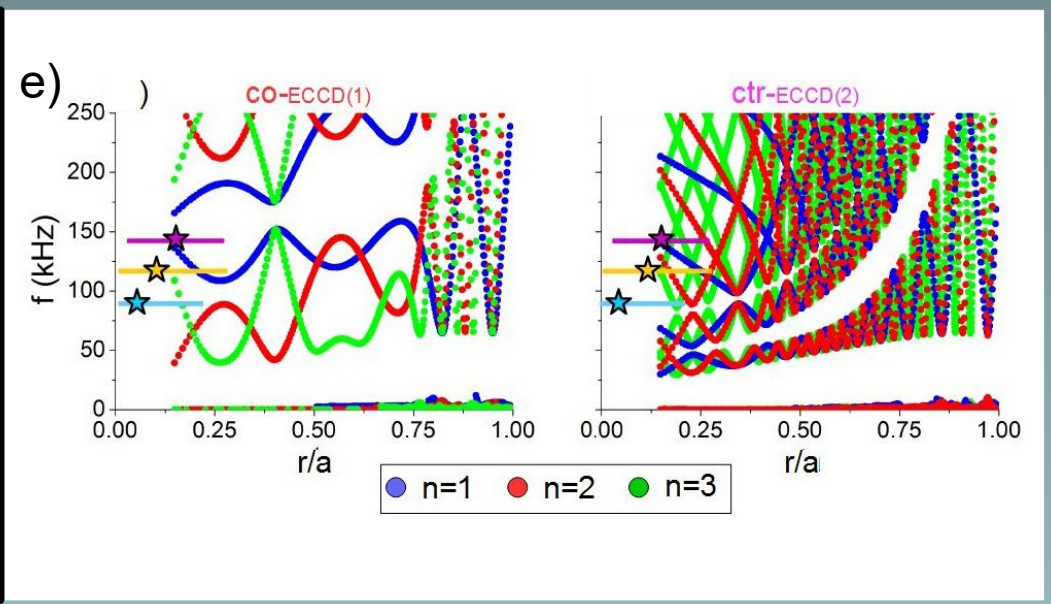

- AEs stable if ctr-ECCD is injected in the plasma (b and d).

- Simulations reproduce the experiment and the unstable AE are identified (a and c).

- **Ctr-ECCD show an improved AE stability because the ECCD iota profiles deformation leads to slender continuum gaps** (e).

J. Varela et al Nucl. Fusion, 60, 112015 (2020)

ECH stabilizes AE in Heliotron J plasma

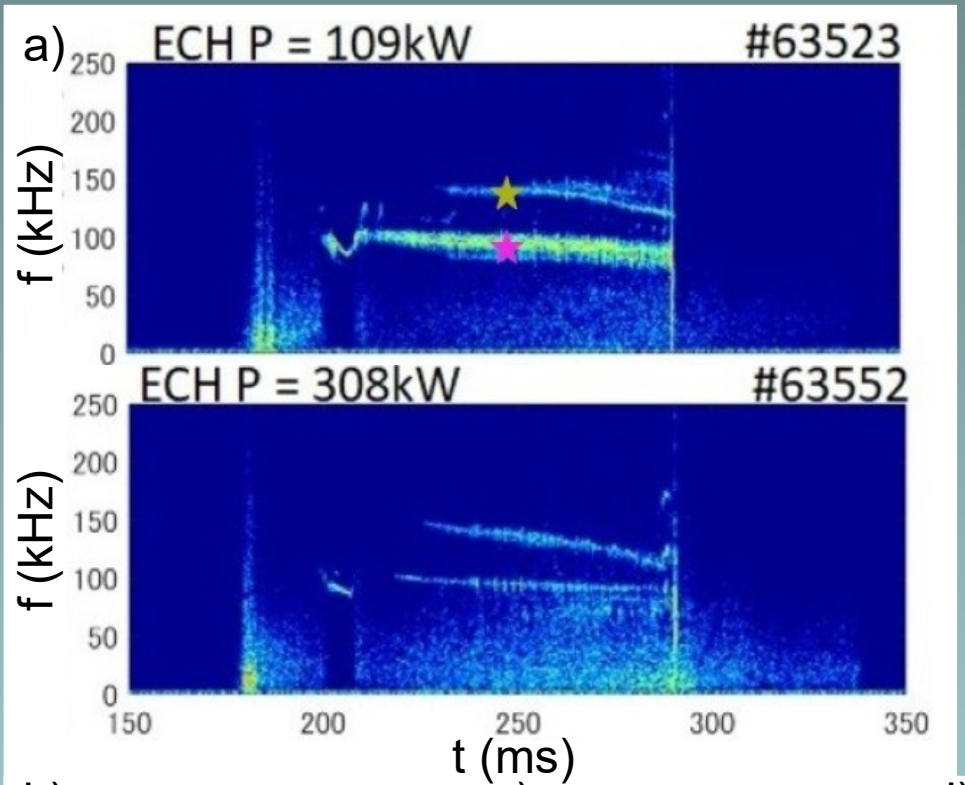

- AE partially stabilized above a given threshold of the ECH injection power (a).

- **AE stabilized by the increase of the thermal ion, e-i Landau and continuum damping !!** (b and c).

- Simulations reproduce the ECH stabilizing effect !! (d and e).

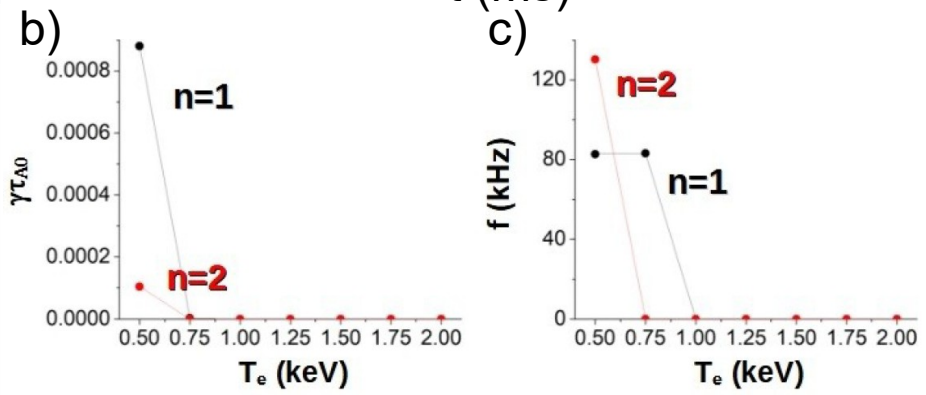

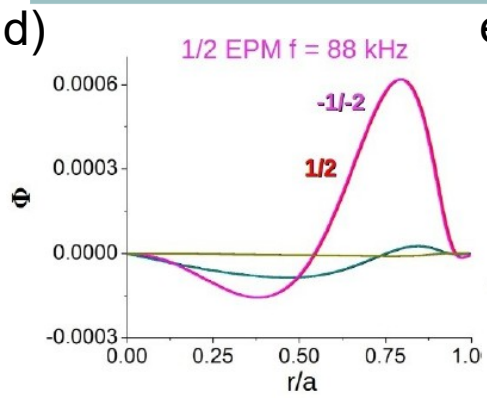

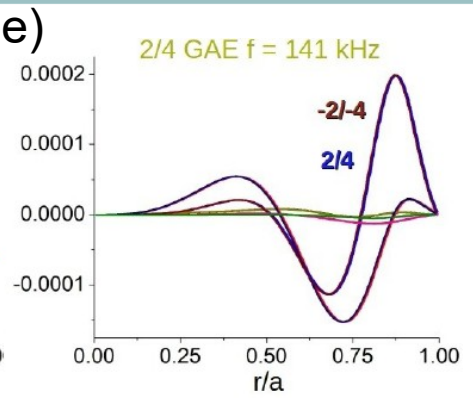

J. Varela et al, 2022 Nucl. Fusion, accepted for publication

EPM stabilization in LHD plasma by ECH injection

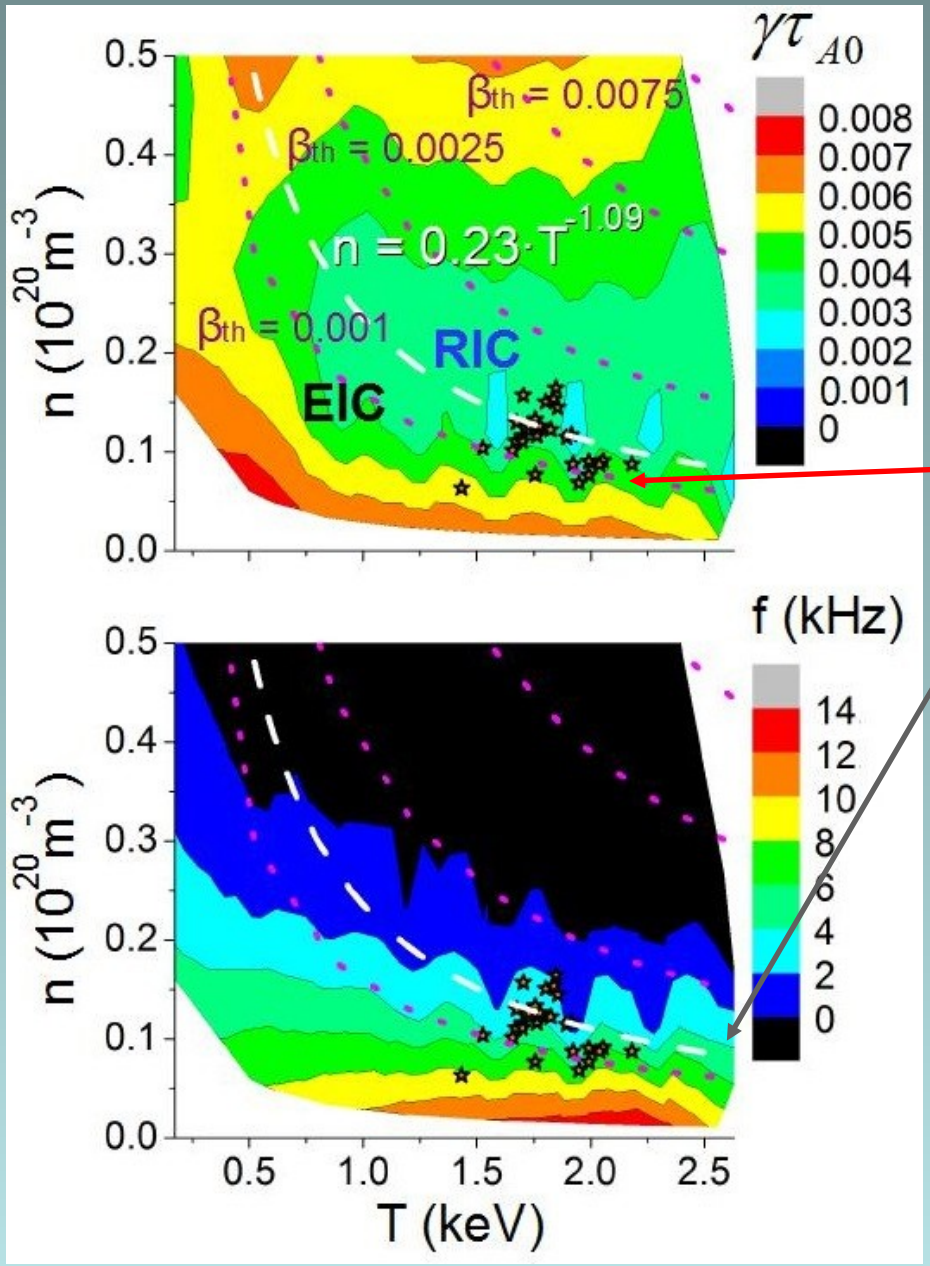

- Stability of Energetic-ion-driven resistive interchange mode (EIC) changes with the plasma density and temperature.

- EIC unstable in plasmas with low density and temperature.

- Plasma density/temperature at iota=1 if EIC unstable. Reasonable agreement between experimental data / simulations.

- Dashed white line: EIC stability threshold vs plasma temperature / density.

$$n = 0.23\,T^{-1.09}$$

- **High density discharges may reduce or avoid the EIC events.**

- **Increase the plasma temperature at the periphery reduces EIC growth rate.**

J. Varela et al, 2020 Nucl. Fusion 60 046013

Analysis of the EIC saturation phase: EIC burst

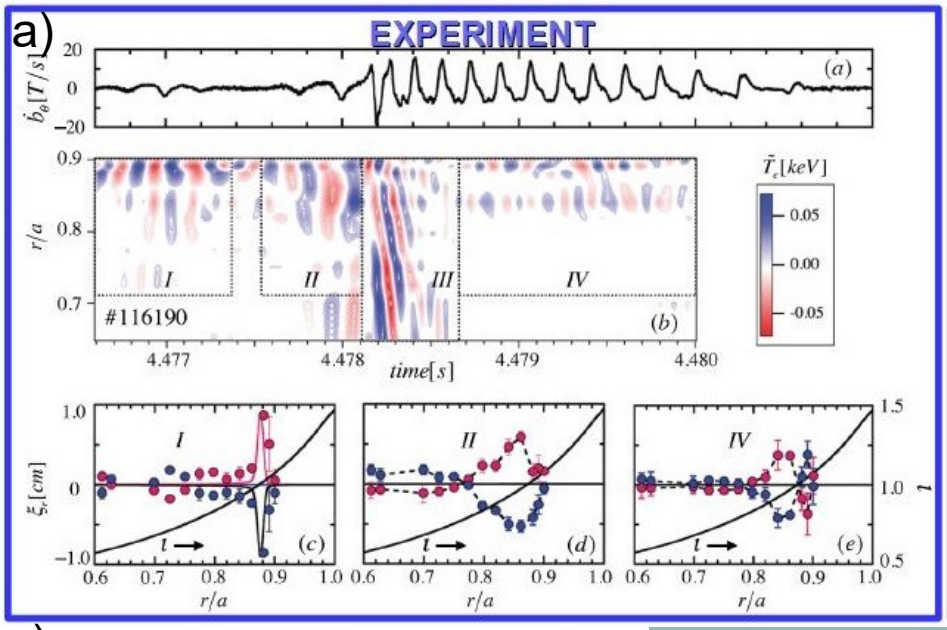

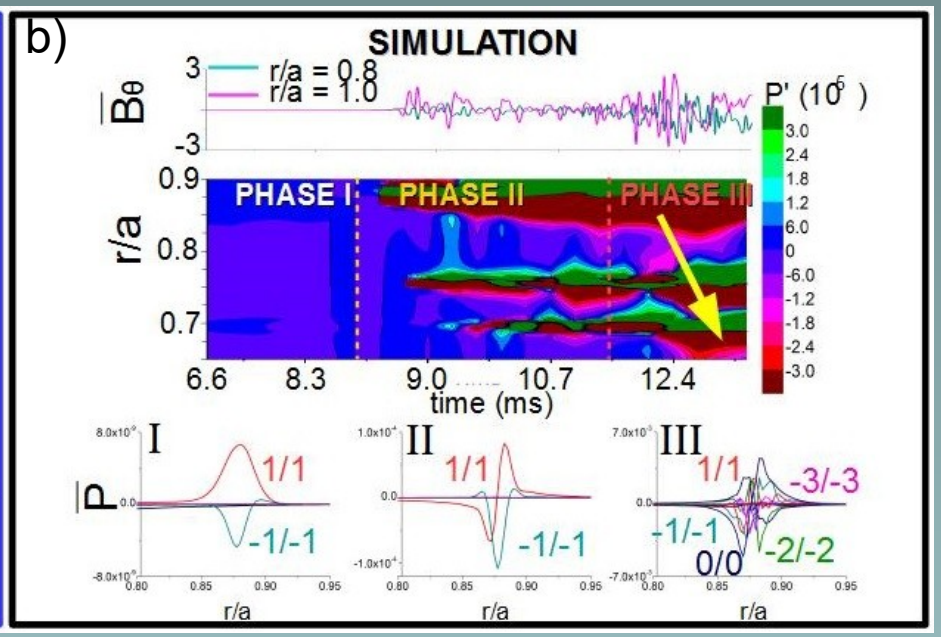

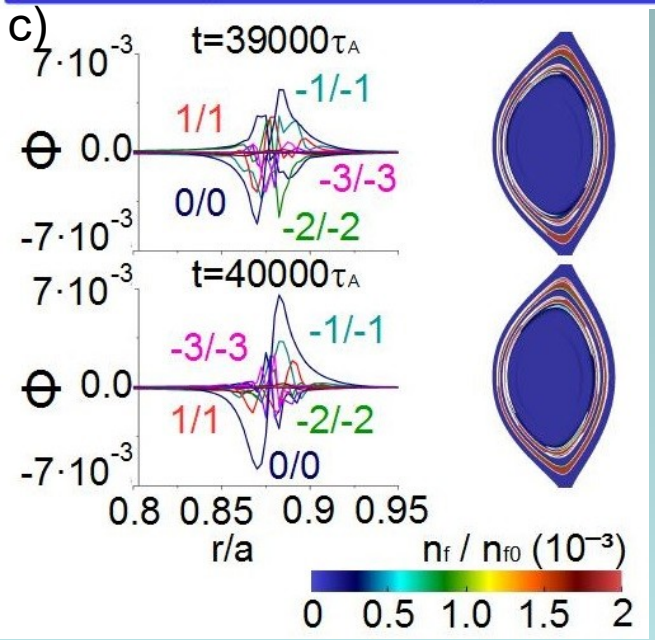

- Bursting observed during the EIC saturation phase leading to large EP losses (a).

- **Simulations indicate the EIC bursting is caused by the 1/1 EIC overlap with 3/4 and 2/3 EPMs (b).**

- EP β threshold, instability frequency range, inwards propagation and complex eigen-function structure consistent with experiment observations (c).

J. Varela et al Nucl. Fusion, 61, 126016 (2021)

TAE saturation in LHD experiment: MHD burst

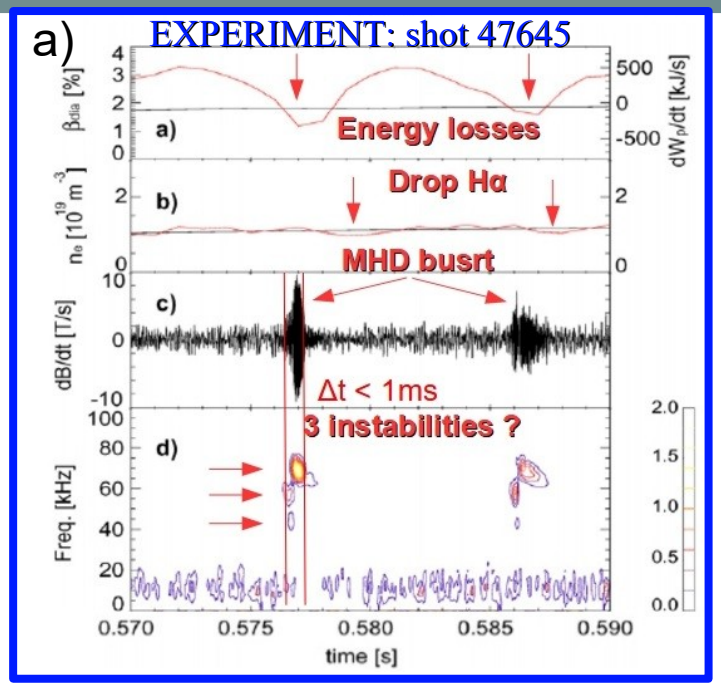

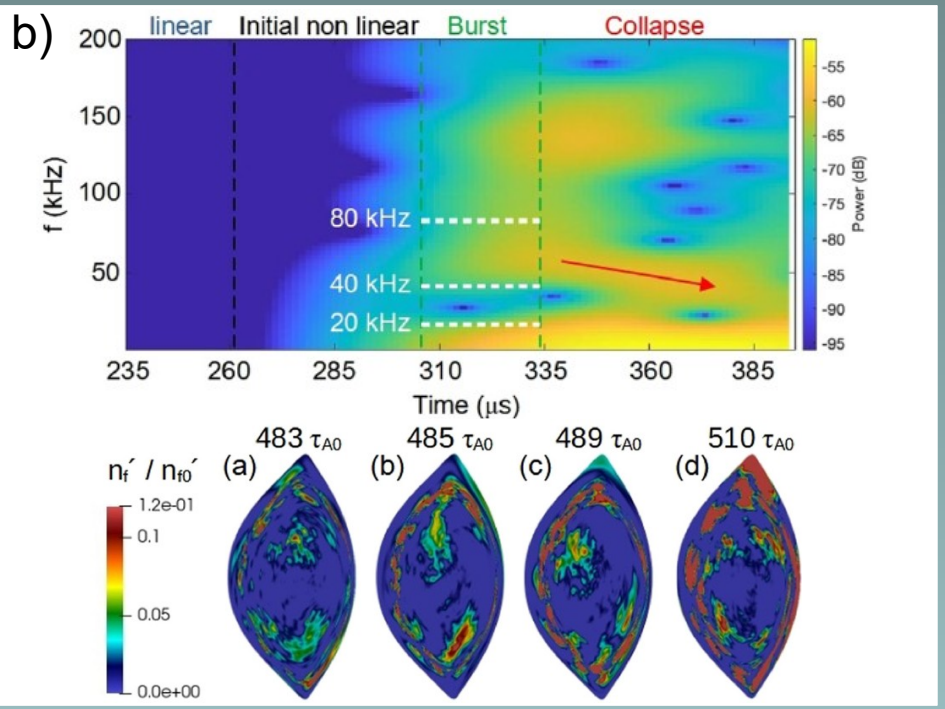

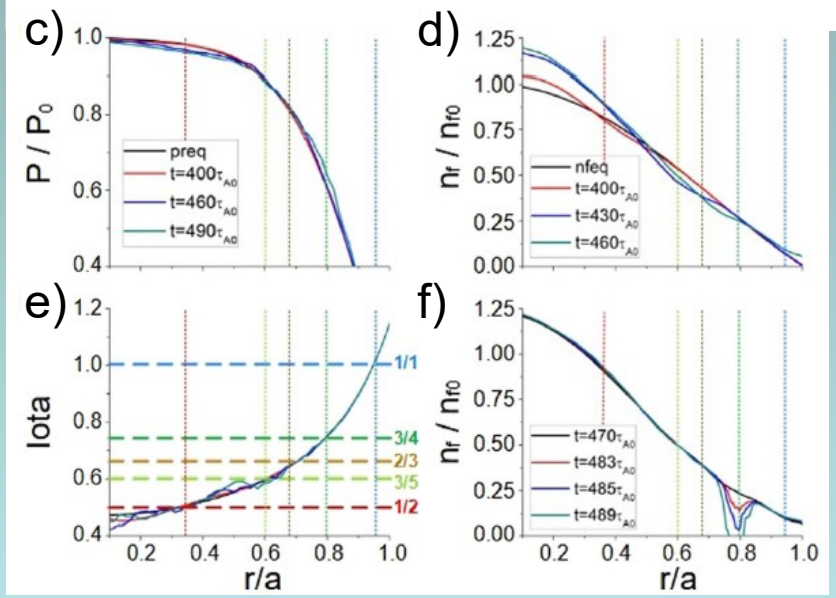

- MHD burst is triggered by three instabilities observed at 45, 55 and 70 kHz (a).
- Simulation indicates the MHD burst is triggered by the resonance overlapping of n=1 to 3 TAEs (b).
- EP population losses at the middle-outer plasma region (f).

J. Varela et al, 2022 Nucl. Fusion 62 126020

Summary

- Several actuators can be used to improve the AE stability in nuclear fusion devices.
- NBCD and ECCD modify the iota profile and the continuum gaps to improve the AE stability: slender continuum gaps leads to improved AE stability.
- An increase of the thermal ion density leads to slender gaps, improving AE stability.
- ECH can stabilize the AEs by increasing the thermal ion FLR, e-i FLR and continuum damping as the electron temperature increases.
- Resonance overlapping during the saturation phase of AE/EPM leads to global relaxation and large EP population losses. Hard MHD limit must be avoided.

CODE DESCRIPTION

FAR3d thermal plasma equations

Toroidal current density

$$J^{\zeta} = \frac{1}{\rho}\frac{\partial}{\partial \rho}\left(-\frac{g_{\rho\theta}}{\sqrt{g}}\frac{\partial \bar{\psi}}{\partial \theta} + \rho\frac{g_{\theta\theta}}{\sqrt{g}}\frac{\partial \bar{\psi}}{\partial \rho}\right) - \frac{1}{\rho}\frac{\partial}{\partial \theta}\left(\frac{g_{\rho\rho}}{\sqrt{g}}\frac{1}{\rho}\frac{\partial \bar{\psi}}{\partial \theta} + \rho\frac{g_{\rho\theta}}{\sqrt{g}}\frac{\partial \bar{\psi}}{\partial \rho}\right)$$

Ion

$$0 = Q - \nabla_{\perp}^2 \bar{\psi}$$

Flow variation along the magnetic field line

Two fluid effects: diamagnetic currents

$$(1)\quad \frac{\partial \psi}{\partial t} = \frac{\partial \Phi}{\partial \zeta} + \iota\frac{\partial \Phi}{\partial \theta} + \frac{\eta}{S}J_{\zeta} + \frac{S}{\varepsilon^2}\frac{B_0\rho_i^2}{(J+\iota I)}\left(\frac{V_A^2}{V_{Te}}\right)\left(\frac{\pi}{2}\right)^{\frac{1}{2}}|\nabla_{\parallel}|Q + \frac{\Lambda S\beta_0}{2\varepsilon^2\omega_{\sigma}\sqrt{g}}\left(\frac{\partial p}{\partial \zeta} + \tau\frac{\partial p}{\partial \theta}\right)$$

$$(2)\quad \frac{\partial U}{\partial t} = \frac{S^2\beta_0}{2\varepsilon^2\rho}\left(\frac{\partial \sqrt{g}}{\partial \theta}\frac{\partial p}{\partial \rho} - \frac{\partial \sqrt{g}}{\partial \rho}\frac{\partial p}{\partial \theta}\right) + S^2\left(\frac{\partial J^{\zeta}}{\partial \zeta} + \iota\frac{\partial J^{\zeta}}{\partial \theta}\right) + \frac{S^2\beta_f}{2\varepsilon^2\rho}\left(\frac{\partial \sqrt{g}}{\partial \theta}\frac{\partial n_f}{\partial \rho} - \frac{\partial \sqrt{g}}{\partial \rho}\frac{\partial n_f}{\partial \theta}\right) + \frac{S^2\beta_{\alpha}}{2\varepsilon^2\rho}\left(\frac{\partial \sqrt{g}}{\partial \theta}\frac{\partial n_{\alpha}}{\partial \rho} - \frac{\partial \sqrt{g}}{\partial \rho}\frac{\partial n_{\alpha}}{\partial \theta}\right)$$

$$+ S\omega_r\rho_i^2\nabla_{\perp}^2 U - S\varepsilon^2\frac{\beta_0 V_{th,f}^3}{\omega_{\sigma}\omega_r}\mathrm{Im}\left[X_e^{//} + X_i^{//} - \frac{(X_i' - X_e')}{2 + X_e + X_i} - \upsilon_i(X_i')^2 - \upsilon_e(X_e')^2\right]\Omega_d^2(\Phi) + \frac{S\beta_0(1-\Lambda)}{2\omega_{\sigma}\varepsilon^2}\left\{\vec{\nabla}\wedge\left[\sqrt{g}\left(\left(\vec{B}\wedge\vec{\nabla}p\right)\cdot\vec{\nabla}\right)\vec{B}_{\perp}\right]\right\}$$

Ion FLR

Pressure gradient driven mode pert.

e-i Landau damping

Toroidal current variation along the magnetic field line

EP density gradient driven mode pert.

Two fluid effects: diamagnetic currents

α density gradient driven mode pert.

FAR3d thermal plasma equations

Advection term

Advection term correction due to the adiabatic index

Acoustic waves: compressibility

Two fluid effects: diamagnetic currents

$$(3)\quad \frac{\partial p}{\partial t} = \frac{dp_{eq}}{d\rho}\frac{1}{\rho}\frac{\partial \Phi}{\partial \theta} + \Gamma p_{eq}\frac{1}{\rho}\left(\frac{\partial}{\partial \rho}\sqrt{g}\frac{\partial \Phi}{\partial \theta} - \frac{\partial}{\partial \theta}\sqrt{g}\frac{\partial \Phi}{\partial \rho}\right) - \frac{\Gamma p_0 B_0}{\varepsilon^2 (J+\iota)}\left(\frac{\partial}{\partial \theta} + \frac{\partial}{\partial \zeta}\right) v_{\parallel,n} + \frac{S\beta_0(1-\Lambda)}{2\omega_c \varepsilon^2 \sqrt{g}}\, p\vec{\nabla} p \cdot \left(\vec{\nabla} \wedge \vec{B}\right)$$

$$(4)\quad \frac{\partial v_{\parallel,n}}{\partial t} = -\frac{S^2 \beta_0 B_0}{\varepsilon^2 n_0 (J+\iota)}\left(\frac{\partial}{\partial \zeta} + \tau\frac{\partial}{\partial \theta}\right) p + \frac{1}{\rho}\frac{\partial \psi}{\partial \theta}\frac{dp_{eq}}{d\rho}$$

Compressibility along magnetic field line

Compressibility due to the poloidal flux angular variation

FAR3d: EP equations

EP density between magnetic field lines

Flow between different magnetic field lines

EP parallel velocity gradient along the magnetic field line

Diamagnetic currents generated by flow between different magnetic field line

$$\frac{\partial n_f}{\partial t} = -\frac{v_{th,f}^2}{\varepsilon^2 \Omega_{cy}} \Omega_d\left(n_f\right) - n_{f0} \nabla_{\parallel} v_{\parallel f} - n_{f0} \Omega_d\left(\Phi\right) - n_{f0} \Omega\left(\Phi\right)$$

$$+\left[\frac{\varepsilon^2 \Omega_{cy}}{v_{th,f}^2} \omega_r n_{f0} - \frac{1}{\rho\left(J+\iota I\right)} \frac{dn_{f0}}{d\rho}\left(I\frac{\partial}{\partial\zeta} - J\frac{\partial}{\partial\theta}\right)\right] W_{NBI}$$

EP FLR

Averaged drift velocity operator passing EP

$$\Omega_d = \frac{1}{2B^4\sqrt{g}}\left[\left(\frac{I}{\rho}\frac{\partial B^2}{\partial\zeta} - J\frac{1}{\rho}\frac{\partial B^2}{\partial\theta}\right)\frac{\partial}{\partial\rho}\right]$$
$$-\frac{1}{2B^4\sqrt{g}}\left[\left(\rho\beta_* \frac{\partial B^2}{\partial\zeta} - J\frac{\partial B^2}{\partial\rho}\right)\frac{1}{\rho}\frac{\partial}{\partial\theta}\right]$$
$$+\frac{1}{2B^4\sqrt{g}}\left[\left(\rho\beta_* \frac{1}{\rho}\frac{\partial B^2}{\partial\theta} - \frac{I}{\rho}\frac{\partial B^2}{\partial\rho}\right)\frac{\partial}{\partial\zeta}\right]$$

Averaged diamagnetic frequency drift

$$\Omega_* = \frac{1}{B^2\sqrt{g}}\frac{1}{n_{f0}}\frac{dn_{f0}}{d\rho}\left(\frac{I}{\rho}\frac{\partial}{\partial\zeta} - J\frac{1}{\rho}\frac{\partial}{\partial\theta}\right)$$

Auxiliary equation

$$0 = (1-(\rho_{f,\alpha})^2\nabla_\perp^2)W^{f,\alpha} - (\rho_{f,\alpha})^2\nabla_\perp^2\tilde{\Phi}$$

FAR3d: EP equations

EP velocity between magnetic field lines

Diamagnetic currents linked to the magnetic field topology

EP density gradient along the magnetic field line

Landau closure: truncate the kinetic moment equation list

$$\frac{\partial v_{\|f}}{\partial t} = -\frac{v_{th,f}^2}{\varepsilon^2 \Omega_{cy}} \Omega_d\left(v_{\|f}\right) - \frac{v_{th,f}^2}{n_{f0}} \nabla_{\|} n_{\|f} + v_{th,f}^2 \Omega\left(\psi\right) - \sqrt{\frac{\pi}{2}} v_{th,f} |\nabla_{\|} v_{\|f}|$$

$$+ \frac{S v_{th,f}^2}{\rho\left(J+\imath I\right)} \frac{1}{n_{f0}} \frac{dn_{f0}}{d\rho} \left(IX_{1,NBI} - JX_{2,NBI}\right)$$

EP FLR

Auxiliary equations

$$0 = (1 - (\rho_{f,\alpha})^2 \nabla_{\perp}^2) X_1^{f,\alpha} - \frac{\partial \bar{\psi}}{\partial \zeta}$$

$$0 = (1 - (\rho_{f,\alpha})^2 \nabla_{\perp}^2) X_2^{f,\alpha} - \frac{\partial \bar{\psi}}{\partial \theta}$$